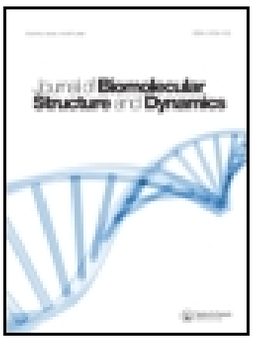

Journal of Biomolecular Structure and Dynamics

ISSN: 0739-1102 (Print) 1538-0254 (Online) Journal homepage: https://www.tandfonline.com/loi/tbsd20

The Effects of Nickel Oxide Nanoparticles on Structural Changes, Heme Degradation, Aggregation of Hemoglobin and Expression of Apoptotic Genes in Lymphocyte Cells

Niusha Abbasi Gamasaee, Hawzheen A Muhammad, Elahe Tadayon, Mahsa Ale-Ebrahim, Mirsasan Mirpour, Majid sharifi, Abbas Salihi, Mudhir Sabir Shekha, Asaad A.B. Alasady, Falah Mohammad Aziz, Keivan Akhtari, Anwarul Hasan & Mojtaba Falahati

To cite this article: Niusha Abbasi Gamasaee, Hawzheen A Muhammad, Elahe Tadayon, Mahsa Ale-Ebrahim, Mirsasan Mirpour, Majid sharifi, Abbas Salihi, Mudhir Sabir Shekha, Asaad A.B. Alasady, Falah Mohammad Aziz, Keivan Akhtari, Anwarul Hasan & Mojtaba Falahati (2019): The Effects of Nickel Oxide Nanoparticles on Structural Changes, Heme Degradation, Aggregation of Hemoglobin and Expression of Apoptotic Genes in Lymphocyte Cells, Journal of Biomolecular Structure and Dynamics, DOI: 10.1080/07391102.2019.1662850

To link to this article: https://doi.org/10.1080/07391102.2019.1662850

Accepted author version posted online: 03 Sep 2019.

The Effects of Nickel Oxide Nanoparticles on Structural Changes, Heme Degradation, Aggregation of Hemoglobin and Expression of Apoptotic Genes in Lymphocyte Cells

Niusha Abbasi Gamasaee[1], Hawzheen A Muhammad[2], Elahe Tadayon[3], Mahsa Ale-Ebrahim[4], Mirsasan Mirpour[5], Majid sharifi[6], Abbas Salihi[7,8,] Mudhir Sabir Shekha[7,9], Asaad A.B. Alasady[10], Falah Mohammad Aziz[7,] Keivan Akhtari[11], Anwarul Hasan[12,13,*], and Mojtaba Falahati[6,*]

[1]Department of Molecular Genetics, Faculty of Advanced Sciences and Technology, Tehran Medical Sciences, Islamic Azad University, Tehran, Iran.

[2]Department of Microbiology, College of Medicine, University of Sulaimani, Sulaimani, Kurdistan Region, Iraq

[3]Faculty of Specialized Veterinary Sciences, Science and Research Branch, Islamic Azad University, Tehran, Iran.

[4]Department of Physiology, Faculty of Advanced Science and Technology, Tehran Medical Sciences, Islamic Azad University, Tehran, Iran

[5]Department of Microbiology, Faculty of Basic Sciences, Lahijan Branch, Islamic Azad University (IAU), Lahijan, Guilan, Iran

[6]Department of Nanotechnology, Faculty of Advanced Sciences and Technology, Tehran Medical Sciences, Islamic Azad University, Tehran, Iran.

[7]Department of Biology, College of Science, Salahaddin University-Erbil, Kurdistan Region, Iraq

[8]Department of Medical Analysis, Faculty of Science, Tishk International University, Erbil, Iraq.

[9]Department of Pathological Analysis, College of Science, Knowledge University, Erbil 074016, Kurdistan Region, Iraq

[10]Anatomy, Histology, and Biology Unit, College of Medicine, University of Duhok, Kurdistan Region, Iraq

[11]Department of Physics, University of Kurdistan, Sanandaj, Iran

[12]Department of Mechanical and Industrial Engineering, College of Engineering, Qatar University, Doha, Qatar

[13]Biomedical Research Centre (BRC), Qatar University– 2713, Doha, Qatar

*Corresponding authors: Anwarul Hasan: ahasan@qu.edu.qa, hasan.anwarul.mit@gmail.com; Mojtaba Falahati: mojtaba.falahati@alumni.ut.ac.ir

Received: 10 July 2019; Revised: 26 August 2019; Accepted: 26 August 2019

Abstract

Nickel oxide nanoparticles (NiO NPs) have received great interests in medical and biotechnological applications. However, their adverse impacts against biological systems have not been well-explored. Herein, the influence of NiO NPs on structural changes, heme degradation and aggregation of hemoglobin (Hb) was evaluated by UV-visible (Vis), circular dichroism (CD), fluorescence, transmission electron microscopy (TEM), and molecular modeling investigations. Also, the morphological changes and expression of Bax/Bcl-2 mRNA in human lymphocyte cell exposed to NiO NPs were assayed by DAPI staining and quantitative real-time PCR (qPCR), respectively. The UV-Vis study depicted that NiO NPs resulted in the displacement of aromatic residues and heme groups and production of the pro-aggregatory species. Intrinsic and Thioflavin T (ThT) fluorescence studies revealed that NiO NPs resulted in heme degradation and amorphous aggregation of Hb, respectively, which the latter result was also confirmed by TEM study. Moreover, far UV-CD study depicted that NiO NPs lead to substantial secondary alteration changes of Hb. Furthermore, near UV-CD displayed that NiO NPs cause quaternary structural changes of Hb as well as heme displacement. Molecular modelling study also approved that NiO NPs resulted in structural changes of Hb and heme deformation. Moreover, morphological and genotoxicity assays revealed that the DNA fragmentation and expression ratio of Bax/Bcl-2 mRNA increased in lymphocyte cells treated with NiO NPs for 24 hr. In conclusion, this study indicates that NiO NPs may affect the biological media and their applications should be limited.

Keywords: Interaction, Nickel oxide, Nanoparticles, Hemoglobin, Heme degradation, Aggregation, Genotoxicity

1. Introduction

Nanoparticles (NPs) have received wide implementations in the industry and biomedical fields. For example, it has been well documented that NPs are used in the sugar industry (Takle *et al.* 2018), footwear industry (Carvalho *et al.* 2018), textile industry (Shahidi 2019), wood industry (Zikeli *et al.* 2018), food industry (Hamad *et al.* 2018), waste water industry (Ismail *et al.* 2019), and gas industry (Peng *et al.* 2018). Furthermore, NPs have been exploiting in drug delivery (Kalimuthu *et al.* 2018; Vallet-Regí *et al.* 2018), cancer therapy (Guimarães *et al.* 2018; Mekheimer *et al.* 2018), neurodegenerative diseases therapy (Vissers *et al.* 2019), antithrombotic therapy (Lee 2018), and diabetes therapy (Rho *et al.* 2018; Ernst *et al.* 2019). Therefore, wide applications of nanomaterial in industry and medicine result in direct human contact with NPs. Internalization of NPs across the cell barrier can result in their interaction with biological macromolecules such as DNA, lipid, and proteins. Therefore, the fate of these NPs following their internalization into the cells and the mechanisms of their induced toxicity demand additional exploration. The basic mechanism proposed for NPs-stimulated protein denaturation and cell mortality is still not well-understood. Indeed, finding the mechanisms behind the toxicity of NPs can hold a great promise to find safe NPs in drug delivery and treatment of several disorders. Nickel oxide (NiO) NPs, one of the most important metal oxides with the cube lattice structure widely used in different areas such as catalysis, gas sensors, battery and magnetic materials (Muñoz & Costa 2012; El-Kemary *et al.* 2013). Due to the physical and chemical properties of NiO NPs, as well as their wide applications in industry, the level of contamination by the NiO NPs in the environment and occupational exposure have been continuously increasing (Hajimohammadjafartehrani *et al.* 2019). Regardless of the factors affecting the toxicity of NiO NPs such as size, shape, charge, and cellular uptake pathways (Ezhilarasi *et al.* 2018), NPs generally increase toxicity by altering protein structure (Chang *et al.* 2017; Ray *et al.* 2018), variation in gene expression (Dumala *et al.* 2017), destroying the cytoplasmic membrane or membranes of intracellular organelles (Ray *et al.* 2018; Sousa *et al.* 2018), stopping chemical intracellular processes (Manna & Bandyopadhyay 2017), and inducing cell death pathways through apoptosis, necrosis, necroptosis, and apoptosis (Siddiqui *et al.* 2012; Abudayyak *et al.* 2017; Ray *et al.* 2018). Therefore, understanding the interactions of NiO NPs with the proteins and cells can provide useful information on the activity of the NiO NPs in the tissues, cells, and even the routes of their uptake to explain the toxicity or beneficial activity of NiO NPs.

The biodistribution of NPs usually results in the interaction of NPs with biological tissues like blood system. Therefore, we aimed to investigate the interaction of NiO NPs with Hb by biophysical and theoretical studies. Afterwards, the morphological changes and genotoxicity of lymphocyte cells induced by NiO NPs were investigated by fluorescence microscopy and molecular assays.

2. Materials and Methods

Hb and NiO NPs (50 nm) were purchased from Sigma-Aldrich Company (USA). All other materials were of analytical grade.

2.1. Protein and nanoparticle solutions preparation

Hb powder was dissolved in phosphate buffer (pH 7.4, 10 mM) and the Hb concentration was determined based on Beer-Lambert law. The NiO powder was also dissolved in phosphate buffer (pH 7.4, 10 mM), vortexed for 15 min followed by water bath at 35°C for 30 min. Afterwards, the concentration of dissolved NPs was obtained using the equation was reported in our previous paper (Rahmani *et al.* 2018).

2.2. UV-Vis study

UV-Vis bands (230-600 nm) of Hb with a concentration of 0.5 mg/ml upon interaction with varying doses of NiO NPs (0.01, 0.05, and 0.1 mg/ml) were determined by Cary Eclipse absorbance spectrophotometer (Varian, Melbourne, Australia) at 25^{o}C to detect the displacement of aromatic residues, solution turbidity, and heme groups triggered by NiO NPs. All protein samples were corrected against buffer and NP solutions.

2.3. Intrinsic fluorescence study

Intrinsic fluorescence spectra of Hb with a concentration of 0.1 mg/ml after interaction with different doses of NiO NPs (0.01, 0.05, and 0.1 mg/ml) were recorded by Cary Eclipse fluorescence spectrophotometer (Varian, Melbourne, Australia) at room temperatures to detect the heme degradation induced by NiO NPs at excitation wavelengths of 325 and 465 nm. Sample preparation and the signal correction were done based on our previous report (Mirzaei *et al.* 2018).

2.4. CD experiments

CD examination was carried out using a spectropolarimeter (model 215, Aviv, Lakewood, NJ, USA). The far-UV CD (190-260 nm) and near –UV CD (250-360 nm and 370-420 nm) bands were recorded at Hb concentration of 0.2 and 1mg/ml, respectively. Protein samples were incubated with increasing concentrations of NiO NPs (0.01, 0.05, and 0.1 mg/ml) at 25°C.

2.5. Simulation methods

The 3D X-ray crystal structures of human normal adult Hb was retrieved from Protein Data Bank (PDB ID: 2H35). A slab with the dimension of 10nm×10nm×1nm was constructed by repeating NiO units. Forcite code and universal force field (UFF) (Rappé *et al.* 1992) were employed to explore the conformational changes and heme deformation of Hb upon interaction with NiO cluster.

2.6. ThT fluorescence assay

ThT fluorescence study was run to monitor the aggregation of Hb molecules incubated with NiO NPs. Hb solution with a fixed dose of 0.1 mg/ml was incubated with varying concentrations of NiO NPs (0.01, 0.05, and 0.1 mg/ml) for 2 min. Afterwards, ThT solution with a final concentration of 15 µM was added to each sample and kept in the dark for 15 min. The samples were then excited at 440 nm, and the emission wavelength was recorded in the range of 460-600 nm.

2.7. TEM investigation

To monitor the morphology of aggregated spices of Hb formed in the presence of NiO NPs, TEM investigation was done based on the procedure reported in our previous paper (Hosseinali *et al.* 2019).

2.8. Cell culture and MTT assay

Lymphocyte cells were freshly prepared and cultured in the cell culture medium, as reported in our previous paper (Babadaei *et al.* 2018). Afterwards, MTT assay was done to calculate the IC_{50} value in the presence of increasing doses of NiO NPs (0, 1, 10, 50, 100 and 200 µg/ml) for 24 hr according to Behzadi *et al.* (2019) study.

2.9. DAPI staining

DAPI staining was used to distinguish the apoptosis cells from normal cells. Briefly, the cells were incubated with increasing doses of NiO NPs (0, 1, 10, 50, 100 and 200 µg/ml) for 24 hr followed by addition of 4% paraformaldehyde for 30 min. DAPI (5 µg/ml) was then added for 15 min and the morphology of nucleus was observed under a fluorescent microscope (Zeiss, Germany).

2.10. qPCR studies

The expression of Bax and Bcl-2 mRNA were explored in lymphocyte cells after treating with IC_{50} concentration of NiO NPs for 24 hr by qPCR investigation based on Babadaei *et al.* (2018) study.

2.10. Statistical analyses

Data extracted from control and incubated samples with NiO NPs were statistically analyzed using one-way ANOVA which was continued by Tukey's comparison test. **P*-value <0.05 was considered statically significant.

3. Results:

3.1. Heme displacement study

UV-Vis spectroscopy was run to monitor the displacement of aromatic residues (Trp, Tyr and Phe) at 280 nm, heme moieties at 408 nm and production of the pro-aggregatory species at 360 nm, after interaction of Hb with increasing doses of NiO NPs. Fig. 1 shows that the three indicated intensities at 280 nm (absorbance of aromatic residues), 360 nm (absorbance of turbid solution) and 408 nm (absorbance of heme groups) increase as the concentration of NiO NPs increases. This data indicated that the conformation of Hb is subjected to some structural changes and displacement of heme groups associated with the protein aggregation. Indeed, it can be indicated that increasing the concentration of NiO NPs, increases the protein unfolding and exposure of the buried hydrophobic

residues particularly in the vicinity of aromatic residues and heme groups that can be reflected in the production of the pro-aggregatory species.

3.2. Heme degradation study

It has been widely documented that degraded spices of heme groups can be excited at around 325 and 465 nm, which emitted the absorbed light at around 462 and 523 nm, respectively (Mirzaei *et al.* 2018). Therefore, in this study, the fluorescence study was carried out to reveal the heme degradation of Hb after interaction with increasing doses of NiO NPs. Fig. 2 shows the fluorescence spectra of Hb in the presence of NiO NPs with different concentrations of 0.01 mg/ml, 0.05 mg/ml, and 0.1 mg/ml as excited at 325 nm (Fig. 2a) and 465 nm (Fig. 2b). As indicated in Fig.2, the intensity of fluorescence spectra at 462 nm and 523 nm enhances, as the concentration of NiO NPs increases, indicating the induction of heme degradation by NiO NPs.

3.3. Structural changes study

Far UV-CD bands were recorded to explore the secondary structure of Hb incubated with different doses of NiO NPs. Fig. 3 depicts the CD bands of free Hb and Hb−NiO NPs complexes. As displayed in Fig. 3, Hb molecules exhibit two negative minima at ∼208 nm ($n\rightarrow\pi^*$) and 222 nm ($\pi\rightarrow\pi^*$), corresponding the α-helical conformation of Hb (Hall *et al.* 2014). In the presence of NiO NPs, it was seen that the ellipticity values of the minima reduced, indicating destabilization of the Hb upon interaction with NiO NPs.

To quantify the structural changes of Hb in the presence of varying concentrations of NiO NPs, CDNN software was used. As tabulated in Table 1, it can be observed that the content of α-helix, β-sheets, turn/ loop, and random coil structure of Hb sample in the absence of NPs as control are calculated to be around 66.32%, 14.88%, 9.21%, and 10.09%, respectively. However, after addition of different concentrations of NiO NPs, the α-helical and β-sheets contents of Hb decreased, whereas the turn/ loop and random coil contents increased. Such substantial reduction in α-helical/ β-sheet content of Hb, upon binding with NiO NPs indicated a considerable structural change in the secondary structure of protein.

Near UV-CD was employed to investigate the quaternary structural changes of Hb in the presence of increasing levels of NiO NPs (0.01 mg/ml, 0.05 mg/ml and 0.1 mg/ml). Fig. 4 shows that as the concentration of NiO NPs increases, the ellipticity changes at 295 nm significantly reduce, whereas the ellipticity changes around 270 nm and 260 nm are not substantial. This data indicates that the NP-induced structural alternations occur around aromatic residues especially Trp counterparts. Indeed, Trp residues displaced to a more hydrophilic environment upon interaction of NiO NPs with Hb. Therefore, it may be concluded that NiO NPs result in secondary and quaternary structural changes of Hb in a dose-dependent fashion.

To more discuss regarding the NiO NPs -mediated structural changes in the Hb (1 mg/ml), heme displacement study was also carried out by near UV-CD technique. As shown in Fig. 5, the maximum ellipticity value at around 412 nm was reduced in the presence of increasing concentrations of NiO NPs. This data exhibits the displacement of heme groups to a more hydrophilic environment. The reason may be due to rearrangement of Hb structure in the presence of NiO NPs as also determined by UV-Vis, far UV-CD bands and near UV-CD (260-340 nm).

3.4. Molecular dynamics study

The NVE ensemble modeled the interaction between Hb and a NiO slab (10 nm × 10 nm × 1 nm) with a time step and simulation time of 1 fs and 100 ps, respectively. The side view of molecular modelling in the beginning and after interaction of Hb with NiO slab is displayed in Fig.6a and Fig. 6b, respectively. Also, the top view in the beginning and after interaction of Hb with NiO nanocluster is shown in Fig. 6c and Fig. 6d, respectively. It can be depicted that by contacting Hb to the NiO surface, NPs stimulate unfolding the quaternary structure of protein molecule and Hb is substantially destabilized in the binding site, which causes a major change in Hb structure. This outcome is also in accordance with UV-Vis and CD results.

Also, it was revealed that NiO cluster upon interaction with Hb results in dynamic porphyrin ring deformation (Fig. 7). This heme deformation induced by NiO NPs may cause heme degradation over time. Indeed, NPs can bind to heme moieties directly or indirectly using different kinds of bonds. In the former case, NPs may induce dynamic heme distortion, whereas in the latter case, NPs may lead to some structural changes around heme groups causing the heme displacement, distortion, deformation, and finally degradation.

3.5. Aggregation assay using fluorescence spectroscopy

The Hb structural changes and subsequent aggregation induced by NiO NPs were explored via ThT fluorescence assay. As shown in Fig. 8, the ThT fluorescence intensity of Hb increased in the presence of varying concentrations of NiO NPs. Therefore, this data may confirm the adverse effects of NiO NPs on structural changes of Hb and corresponding aggregation.

3.6. TEM study

TEM investigation was performed to monitor the morphology of aggregated species of Hb incubated with NiO NPs (0.1 mg/ml) for 2 min. Fig 9 a, b and c represent the Hb molecules, NiO NP molecules and NiO/Hb complex, respectively. As shown in Fig. 9a, Hb molecules show a well-dispersed morphology and do not tend to be aggregated. Fig. 9b exhibits the spherical shape of NiO NPs with an average diameter of around 50 nm. Fig.9 c, depicts that Hb molecules aggregated in the form of amorphous species around NiO NPs. Indeed, NiO NPs resulted in structural changes and respective aggregation of Hb.

3.7. Viability assay

Viability data revealed dose-dependent toxicity of NiO NPs on lymphocyte cells (Fig. 10). The MTT assay was done after incubating lymphocyte cells with NiO NPs cells for 24 hr. NiO NPs with doses of 1 µg/ml, 10µg/ml, 50µg/ml, 100µg/ml, and 200 µg/ml resulted in the reduction of cell viability to 93.24%±15.40, 90.56%±15.40, 83.33%±8.08, 46.32%±7.11, and 40.97%±5.0, respectively. The IC_{50} of NiO NPs was calculated to be 95µg/ml.

3.8. Morphological assay

The morphological changes stimulated by varying concentrations of NiO NPs were assessed in the DAPI assay by fluorescence microscopy (Figure 11). The DAPI staining depicted that control cells (Figure 11A) and treated cells by NPs with concentrations of 1 µg/ml (Figure 11B) and 10 µg/ml (Figure 11C) show almost dark blue appearance, indicating the presence of normal and viable cells. However, after incubation of cells with higher concentrations of NiO: i.e., 50 µg/ml (Figure 11D), 100 µg/ml (Figure 11E), and 200 µg/ml (Figure 11F), significant bright appearance having nuclear condensation and DNA fragmentation were observed, which these NP-induced morphological changes was more pronounced for higher concentration of NPs than lower ones.

3.8. Genotoxicity assay

To explore if NiO NPs trigger apoptosis in lymphocyte cells, the expression of Bcl-2 and Bax mRNA were investigated by qPCR analysis after 24 hr incubation with IC_{50} concentration of NiO NPs. The relative expression of Bax was up-regulated to 1.21 unit relative to control group, (**P*-value <0.05), whereas the relative expression of Bcl-2 was down-regulated to 0.85 unit relative to control group, (**P*-value <0.05) (Fig. 12). Afterwards, the expression ratio of Bax/Bcl-2 mRNA was calculated, since this ratio is important for revealing the apoptosis induced by toxic agents. As shown in Fig.12, the expression ratio of Bax/Bcl-2 mRNA increased to 1.42 unit in lymphocyte cells in the presence of NiO NPs (**P*-value <0.05).

4. Discussion

Study on the toxicity of NPs has evolved into a crucial concern in biochemistry and biophysics. Concerning medical applications, NPs have conclusively passed into the area, developing the field of nanomedicine where NPs are exploited for drug delivery, diagnosis, and therapy. Besides these activities, researchers have concerned the selective approaches in which NPs interact with biomolecules like proteins. We found that NiO NPs results in secondary and quaternary structural changes of Hb. Regarding the structural changes of proteins; some other reports have been published. For example, Zolghadri *et al.* (2009) and Gebauer *et al.* (2012) showed that human serum albumin (HSA) and Hb molecules as protein corona are denatured after adsorption on the surface of silver (Ag) NPs to some extent. Mehdizadeh *et al.* (2019) also revealed that NiO NPs result in conformational changes of tau protein from a natively disordered structure toward a more folded structure. However, Esfandfar *et al.* (2016) revealed that copper oxide (CuO) NPs do not stimulate profound structural changes in the structure of HSA. Also, Aghili *et al.* (2016) depicted that iron NPs do not induce remarkable changes in the lysozyme structure. Therefore, depending on the dimension, morphology, functional groups, hydrophilic properties, and intrinsic stability of proteins, engineered NPs can react in the different ways with biomolecules like proteins. For example, Lundqvist *et al.* (2004) demonstrated that conformational variation of human carbonic anhydrase immobilized onto silica (SiO_2) NPs depend on the NP geometry and the intrinsic protein stability. Shang *et al.* (2009) also revealed that the interaction of cytochrome c with SiO_2 NPs and subsequent structural variations and enzymatic activity depends on NP dimension. Falahati *et al.* (2012) also revealed that modification of mesoporous SiO_2 NPs with positive moieties influence the interaction mechanism and stability of confined biomolecule.

Satzer *et al.* (2016) also reported that by interactions of nine different biomolecules with SiO_2NPs, only bovine serum albumin (BSA) and myoglobin underwent structural changes, and the NP-induced conformational changes were correlated with the NP dimension. Indeed, structural alterations were detected only for NPs larger than 150 nm. In another study, Vitali *et al.* (2018) compared the structural changes of intrinsically disordered proteins with lysozyme upon interaction with NPs. They found that intrinsically disordered proteins did not show a substantial structural changes upon interaction with SiO_2 NPs, whereas lysozyme did not preserve its helical structures (Vitali *et al.* 2018). They also reported that NPs promoted α-synuclein amyloid formation in a concentration-dependent manner.

Also, we found that heme degradation of Hb occurs after interaction with NiO NPs. It has also been reported that cerium oxide NPs (Mobasherat Jajroud *et al.* 2018) and iron NPs (Mirzaei *et al.* 2018) can cause heme degradation in a concentration-dependent manner.

In this paper, we also revealed that NiO NPs results in the aggregation of Hb molecules into the amorphous species. Actually, by doing UV-Vis spectroscopy and exploring the absorption intensity

at 360 nm as a criterion for the amorphous aggregation of protein, it was observed that the intensity of Hb molecules enhances as the concentration of NiO NP increases. Also, far and near UV-CD showed that the secondary and quaternary structures of protein were substantially changed from a folded structure toward a more random coil conformation. TEM study and ThT assay also revealed the formation of pro-aggregatory species after interaction of Hb with NiO NPs. In this paper, we incubated Hb with different concentrations of NPs for 2 min. However, it was found that the incubation time of 2 hr had no significant effect on the ThT fluorescence intensity or CD signal of Hb molecules in the presence of NiO NPs compared to incubation time of 2 min (data not shown). Indeed, the effect of incubation time on the aggregation tendency of large molecules like Hb should be explored in the amyloidogenic conditions, whereas in our study Hb was dissolved in a normal phosphate buffer with a pH 7.4. Therefore, in the future studies, the Hb molecules can be dissolved in amyloidogenic buffers having acidic or basic pH with high ionic strength to induce the formation of amyloid like fibrils of Hb and explore the inhibitory or activatory effects of NiO NPs on the kinetic pathways of aggregation.

Zeinabad *et al.* (2016) also manifested that carbon nanotube [single wall (SW) or multiwall (MW)] with different diameters and morphologies have different effects in tau structure. Indeed, it was shown that amorphous aggregation of tau was more triggered by MWCNTs relative to SWCNTs (Zeinabad *et al.* 2016) after 2 min of incubation.

Regarding cellular assays, we found that NiO NPs only with high concentration can stimulate cell mortality. Indeed, NiO NPs with an IC_{50} of 95 μg/ml can up-regulate the expression of Bax mRNA and down-regulate the expression of Bcl-2 mRNA, as apoptotic and antiapoptotic genes, respectively.

Ye *et al.* (2010) reported that SiO_2 NPs triggered apoptosis via upregulation of apoptotic gens induced by oxidative stress in human hepatic cells. Ahamed *et al.* (2011) revealed that zinc oxide (ZnO) nanorod stimulated cell mortality and apoptosis via Bax/Bcl-2 pathways. Assadian *et al.* (2018) reported the cytotoxicity of CuO NPs and Fe_2O_3 NPs on lymphocytes cells. They revealed that both NPs, increased the cell mortality with a remarkable enhance at intracellular ROS value and loss of mitochondrial dysfunction (Assadian *et al.* 2018). Recently, NiO NPs were found to target endoplasmic reticulum and mitochondria in rat renal tubular cells (Abdulqadir & Aziz 2019). The toxicity of titanium oxide (TiO_2) NPs (Kang *et al.* 2008; Kang *et al.* 2011; Ghosh *et al.* 2013; Aliakbari *et al.* 2019), cobalt NPs (Rajiv *et al.* 2016), Fe_3O_4 NPs (Rajiv *et al.* 2016), SiO_2 NPs (Rajiv *et al.* 2016; Sabziparvar *et al.* 2018), and zero-valent iron NPs (Asl *et al.* 2018) against lymphocyte cells have been also reported. Indeed, the qPCR assay has been widely used to monitor the variation in the Bax and Bcl-2 mRNA expression for evaluation of cytotoxicity of NPs. For instance, it has been documented that SiO_2 NPs (Ye *et al.* 2010), ZnO nanorod (Ahamed *et al.* 2011), TiO_2 NPs (Zhu *et al.* 2012), fullerene (Song *et al.* 2012), ZnO NPs (Liang *et al.* 2016), gadolinium oxide NPs (Alarifi *et al.* 2017), and Ag/gold (Au) bimetallic NPs (Katifelis *et al.* 2018) induce cell mortality in cell lines via Bax/Bcl-2 pathways.

The NP-induced cell mortality also depends on physicochemical features of NPs. Indeed, unlimited modification of NPs with different moieties and tuning the morphology and size of NPs can be used for the modulation of the NP toxicity (Hofmann-Amtenbrink *et al.* 2015). The attachment of proteins to NPs is also influenced the NP internalization into the cells and subsequent toxicity (Aggarwal *et al.* 2009).

5. Conclusion

Herein, the impact of NiO NPs on conformational alterations, heme degradation and aggregation of Hb was evaluated by different techniques. Moreover, the genotoxicity of NiO NPs on human

lymphocyte cell was assayed by qPCR assay. The spectroscopic and theoretical analysis revealed that NiO NPs resulted in secondary and quaternary structural changes of Hb, heme degradation, and aggregation of Hb. Moreover, cellular and genotoxicity assay showed that the DNA fragmentation and expression ratio of Bax/Bcl-2 mRNA increased in lymphocyte cells incubated with IC_{50} doses of NiO NPs for 24 hr. Exploring the reaction of NPs with a biological system is required to realize the behavior of biomolecules in contact with NPs. All chemical data must live up to the "biological systems", first *in vitro* and finally *in vivo*, to help us to develop a brand-new system for promising therapeutic approaches.

Conflicts of interest

The authors have none to declare.

Acknowledgment

This article was made possible by the grant NPRP10-120-170-211 from Qatar national Research Fund (a part of Qatar Foundation). All statements here are the sole responsibility of the authors.

References

Abdulqadir, S. Z. & Aziz, F. M. (2019). Internalization and effects on cellular ultrastructure of nickel nanoparticles in rat kidneys. *International journal of nanomedicine 14*: 3995.

Abudayyak, M., Guzel, E. & Özhan, G. (2017). Nickel oxide nanoparticles are highly toxic to SH-SY5Y neuronal cells. *Neurochemistry International 108*: 7-14.

Aggarwal, P., Hall, J. B., McLeland, C. B., Dobrovolskaia, M. A. & McNeil, S. E. (2009). Nanoparticle interaction with plasma proteins as it relates to particle biodistribution, biocompatibility and therapeutic efficacy. *Advanced drug delivery reviews 61*: 428-437.

Aghili, Z., Taheri, S., Zeinabad, H. A., Pishkar, L., Saboury, A. A., Rahimi, A. & Falahati, M. (2016). Investigating the interaction of Fe nanoparticles with lysozyme by biophysical and molecular docking studies. *PloS one 11*: 0164878-88.

Ahamed, M., Akhtar, M. J., Raja, M., Ahmad, I., Siddiqui, M. K. J., AlSalhi, M. S. & Alrokayan, S. A. (2011). ZnO nanorod-induced apoptosis in human alveolar adenocarcinoma cells via p53, survivin and bax/bcl-2 pathways: role of oxidative stress. *Nanomedicine: Nanotechnology, Biology and Medicine 7*: 904-913.

Alarifi, S., Ali, H. & Saad Alkahtani, M. S. A. (2017). Regulation of apoptosis through bcl-2/bax proteins expression and DNA damage by nano-sized gadolinium oxide. *International journal of nanomedicine 12*: 4541-55.

Aliakbari, F., Haji Hosseinali, S., Khalili Sarokhalil, Z., Shahpasand, K., Akbar Saboury, A., Akhtari, K. & Falahati, M. (2019). Reactive oxygen species generated by titanium oxide nanoparticles stimulate the hemoglobin denaturation and cytotoxicity against human lymphocyte cell. *Journal of Biomolecular Structure and Dynamics*1: 1-7.

Asl, B. A., Mogharizadeh, L., Khomjani, N., Rasti, B., Pishva, S. P., Akhtari, K., Attar, F. & Falahati, M. (2018). Probing the interaction of zero valent iron nanoparticles with blood system by

biophysical, docking, cellular, and molecular studies. *International journal of biological macromolecules 109*: 639-650.

Assadian, E., Zarei, M. H., Gilani, A. G., Farshin, M., Degampanah, H. & Pourahmad, J. (2018). Toxicity of copper oxide (CuO) nanoparticles on human blood lymphocytes. *Biological trace element research 184*: 350-357.

Babadaei, M. M. N., Moghaddam, M. F., Solhvand, S., Alizadehmollayaghoob, E., Attar, F., Rajabbeigi, E., Akhtari, K., Sari, S. & Falahati, M. (2018). Biophysical, bioinformatical, cellular, and molecular investigations on the effects of graphene oxide nanosheets on the hemoglobin structure and lymphocyte cell cytotoxicity. *International journal of nanomedicine 13*: 6871-77.

Behzadi, E., Sarsharzadeh, R., Nouri, M., Attar, F., Akhtari, K., Shahpasand, K. & Falahati, M. (2019). Albumin binding and anticancer effect of magnesium oxide nanoparticles. *International journal of nanomedicine 14*: 257-267.

Carvalho, I., Ferdov, S., Mansilla, C., Marques, S., Cerqueira, M., Pastrana, L., Henriques, M., Gaidau, C., Ferreira, P. & Carvalho, S. (2018). Development of antimicrobial leather modified with Ag–TiO2 nanoparticles for footwear industry. *Science and Technology of Materials 30*: 60-68.

Chang, X., Zhu, A., Liu, F., Zou, L., Su, L., Liu, S., Zhou, H., Sun, Y., Han, A. & Sun, Y. (2017). Nickel oxide nanoparticles induced pulmonary fibrosis via TGF-β 1 activation in rats. *Human & Experimental Toxicology 36*: 802-812.

Dumala, N., Mangalampalli, B., Chinde, S., Kumari, S. I., Mahoob, M., Rahman, M. F. & Grover, P. (2017). Genotoxicity study of nickel oxide nanoparticles in female Wistar rats after acute oral exposure. *Mutagenesis 32*: 417-427.

El-Kemary, M., Nagy, N. & El-Mehasseb, I. (2013). Nickel oxide nanoparticles: synthesis and spectral studies of interactions with glucose. *Materials Science in Semiconductor Processing 16*: 1747-1752.

Ernst, A. U., Bowers, D. T., Wang, L.-H., Shariati, K., Plesser, M. D., Brown, N. K., Mehrabyan, T. & Ma, M. (2019). Nanotechnology in cell replacement therapies for type 1 diabetes. *Advanced drug delivery reviews* 1:1-10

Esfandfar, P., Falahati, M. & Saboury, A. (2016). Spectroscopic studies of interaction between CuO nanoparticles and bovine serum albumin. *Journal of Biomolecular Structure and Dynamics 34*: 1962-1968.

Ezhilarasi, A. A., Vijaya, J. J., Kaviyarasu, K., Kennedy, L. J., Ramalingam, R. J. & Al-Lohedan, H. A. (2018). Green synthesis of NiO nanoparticles using Aegle marmelos leaf extract for the evaluation of in-vitro cytotoxicity, antibacterial and photocatalytic properties. *Journal of Photochemistry and Photobiology B: Biology 180*: 39-50.

Falahati, M., Saboury, A. A., Ma'mani, L., Shafiee, A. & Rafieepour, H. A. (2012). The effect of functionalization of mesoporous silica nanoparticles on the interaction and stability of confined enzyme. *International journal of biological macromolecules 50*: 1048-1054.

Gebauer, J. S., Malissek, M., Simon, S., Knauer, S. K., Maskos, M., Stauber, R. H., Peukert, W. & Treuel, L. (2012). Impact of the nanoparticle–protein corona on colloidal stability and protein structure. *Langmuir 28*: 9673-9679.

Ghosh, M., Chakraborty, A. & Mukherjee, A. (2013). Cytotoxic, genotoxic and the hemolytic effect of titanium dioxide (TiO2) nanoparticles on human erythrocyte and lymphocyte cells in vitro. *Journal of applied toxicology 33*: 1097-1110.

Guimarães, P. P., Gaglione, S., Sewastianik, T., Carrasco, R. D., Langer, R. & Mitchell, M. J. (2018). Nanoparticles for immune cytokine TRAIL-based cancer therapy. *ACS nano 12*: 912-931.

Hajimohammadjafartehrani, M., Hosseinali, S. H., Dehkohneh, A., Ghoraeian, P., Ale-Ebrahim, M., Akhtari, K., Shahpasand, K., Saboury, A. A., Attar, F. & Falahati, M. (2019). The effects of nickel oxide nanoparticles on tau protein and neuron-like cells: Biothermodynamics and molecular studies. *International Journal of Biological Macromolecules 127*: 330-339.

Hall, V., Nash, A. & Rodger, A. (2014). SSNN, a method for neural network protein secondary structure fitting using circular dichroism data. *Analytical Methods 6*: 6721-6726.

Hamad, A. F., Han, J.-H., Kim, B.-C. & Rather, I. A. (2018). The intertwine of nanotechnology with the food industry. *Saudi journal of biological sciences 25*: 27-30.

Hofmann-Amtenbrink, M., Grainger, D. W. & Hofmann, H. (2015). Nanoparticles in medicine: Current challenges facing inorganic nanoparticle toxicity assessments and standardizations. *Nanomedicine: Nanotechnology, Biology and Medicine 11*: 1689-1694.

Hosseinali, S. H., Boushehri, Z. P., Rasti, B., Mirpour, M., Shahpasand, K. & Falahati, M. (2019). Biophysical, molecular dynamics and cellular studies on the interaction of nickel oxide nanoparticles with tau proteins and neuron-like cells. *International Journal of Biological Macromolecules 125*: 778-784.

Ismail, I., Balachandran, S. & Devi, M. G. (2019). Synthesis, characterization and application of nanoparticles in wastewater treatment. *Indian Chemical Engineer 61*: 77-86.

Kalimuthu, K., Lubin, B.-C., Bazylevich, A., Gellerman, G., Shpilberg, O., Luboshits, G. & Firer, M. A. (2018). Gold nanoparticles stabilize peptide-drug-conjugates for sustained targeted drug delivery to cancer cells. *Journal of nanobiotechnology 16*: 34-40.

Kang, S. J., Kim, B. M., Lee, Y. J. & Chung, H. W. (2008). Titanium dioxide nanoparticles trigger p53-mediated damage response in peripheral blood lymphocytes. *Environmental and molecular mutagenesis 49*: 399-405.

Kang, S. J., Lee, Y. J., Kim, B. M., Choi, Y. J. & Chung, H. W. (2011). Cytotoxicity and genotoxicity of titanium dioxide nanoparticles in UVA-irradiated normal peripheral blood lymphocytes. *Drug and chemical toxicology 34*: 277-284.

Katifelis, H., Lyberopoulou, A., Mukha, I., Vityuk, N., Grodzyuk, G., Theodoropoulos, G. E., Efstathopoulos, E. P. & Gazouli, M. (2018). Ag/Au bimetallic nanoparticles induce apoptosis in human cancer cell lines via P53, CASPASE-3 and BAX/BCL-2 pathways. *Artificial cells, nanomedicine, and biotechnology 46*: S389-S398.

Lee, D. (2018). Theranostic nanoparticles for Thrombosed Vessels: H2O2-Activatable Contrast-Enhanced Photoacoustic Imaging and Antithrombotic Therapy. *Circulation Research 123*: A299-A299.

Liang, S., Sun, K., Wang, Y., Dong, S., Wang, C., Liu, L. & Wu, Y. (2016). Role of Cyt-C/caspases-9, 3, Bax/Bcl-2 and the FAS death receptor pathway in apoptosis induced by zinc oxide nanoparticles in human aortic endothelial cells and the protective effect by alpha-lipoic acid. *Chemico-biological interactions 258*: 40-51.

Lundqvist, M., Sethson, I. & Jonsson, B.-H. (2004). Protein adsorption onto silica nanoparticles: conformational changes depend on the particles' curvature and the protein stability. *Langmuir 20*: 10639-10647.

Manna, I. & Bandyopadhyay, M. (2017). Engineered nickel oxide nanoparticle causes substantial physicochemical perturbation in plants. *Frontiers in chemistry 5*: 92-100.

Mehdizadeh, P., Fesharaki, S. S. H., Nouri, M., Ale-Ebrahim, M., Akhtari, K., Shahpasand, K., Saboury, A. A. & Falahati, M. (2019). Tau folding and cytotoxicity of neuroblastoma cells in the presence of manganese oxide nanoparticles: Biophysical, molecular dynamics, cellular, and molecular studies. *International journal of biological macromolecules 125*: 674-682.

Mekheimer, K. S., Hasona, W., Abo-Elkhair, R. & Zaher, A. (2018). Peristaltic blood flow with gold nanoparticles as a third grade nanofluid in catheter: Application of cancer therapy. *Physics Letters A 382*: 85-93.

Mirzaei, S., Hadadi, Z., Attar, F., Mousavi, S. E., Zargar, S. S., Tajik, A., Saboury, A. A., Rezayat, S. M. & Falahati, M. (2018). ROS-mediated heme degradation and cytotoxicity induced by iron nanoparticles: Hemoglobin and lymphocyte cells as targets. *Journal of Biomolecular Structure and Dynamics 36*: 4235-4245.

Mobasherat Jajroud, S. Y., Falahati, M., Attar, F. & Khavari-Nejad, R. A. (2018). Human hemoglobin adsorption onto colloidal cerium oxide nanoparticles: a new model based on zeta potential and spectroscopy measurements. *Journal of Biomolecular Structure and Dynamics 36*: 2908-2916.

Muñoz, A. & Costa, M. (2012). Elucidating the mechanisms of nickel compound uptake: a review of particulate and nano-nickel endocytosis and toxicity. *Toxicology and Applied Pharmacology 260*: 1-16.

Peng, B., Tang, J., Luo, J., Wang, P., Ding, B. & Tam, K. C. (2018). Applications of nanotechnology in oil and gas industry: Progress and perspective. *The Canadian Journal of Chemical Engineering 96*: 91-100.

Rahmani, S., Mogharizadeh, L., Attar, F., Rezayat, S. M., Mousavi, S. E., & Falahati, M. (2018). Probing the interaction of silver nanoparticles with tau protein and neuroblastoma cell line as nervous system models. *Journal of Biomolecular Structure and Dynamics* 36(15): 4057-4071.

Rajiv, S., Jerobin, J., Saranya, V., Nainawat, M., Sharma, A., Makwana, P., Gayathri, C., Bharath, L., Singh, M. & Kumar, M. (2016). Comparative cytotoxicity and genotoxicity of cobalt (II, III) oxide, iron (III) oxide, silicon dioxide, and aluminum oxide nanoparticles on human lymphocytes in vitro. *Human & experimental toxicology 35*: 170-183.

Rappé, A. K., Casewit, C. J., Colwell, K., Goddard III, W. A. & Skiff, W. (1992). UFF, a full periodic table force field for molecular mechanics and molecular dynamics simulations. *Journal of the American Chemical Society 114*: 10024-10035.

Ray, S. K., Dhakal, D., Regmi, C., Yamaguchui, T. & Lee, S. W. (2018). Inactivation of Staphylococcus aureus in visible light by morphology tuned α-NiMoO4. *Journal of Photochemistry and Photobiology A: Chemistry 350*: 59-68.

Rho, J. G., Han, H. S., Han, J. H., Lee, H., Lee, W. H., Kwon, S., Heo, S., Yoon, J., Shin, H. H. & Lee, E.-y. (2018). Self-assembled hyaluronic acid nanoparticles: Implications as a nanomedicine for treatment of type 2 diabetes. *Journal of Controlled Release 279*: 89-98.

Sabziparvar, N., Saeedi, Y., Nouri, M., Najafi Bozorgi, A. S., Alizadeh, E., Attar, F., Akhtari, K., Mousavi, S. E. & Falahati, M. (2018). Investigating the interaction of silicon dioxide nanoparticles with human hemoglobin and lymphocyte cells by biophysical, computational, and cellular studies. *The Journal of Physical Chemistry B 122*: 4278-4288.

Satzer, P., Svec, F., Sekot, G. & Jungbauer, A. (2016). Protein adsorption onto nanoparticles induces conformational changes: particle size dependency, kinetics, and mechanisms. *Engineering in life sciences 16*: 238-246.

Shahidi, S. (2019). Magnetic nanoparticles application in the textile industry—A review. *Journal of Industrial Textile* 1: 1-10.

Shang, W., Nuffer, J. H., Muñiz-Papandrea, V. A., Colón, W., Siegel, R. W. & Dordick, J. S. (2009). Cytochrome c on silica nanoparticles: influence of nanoparticle size on protein structure, stability, and activity. *Small 5*: 470-476.

Siddiqui, M. A., Ahamed, M., Ahmad, J., Majeed Khan, M. A., Musarrat, J., Al-Khedhairy, A. A. & Alrokayan, S. A. (2012). Nickel oxide nanoparticles induce cytotoxicity, oxidative stress and apoptosis in cultured human cells that is abrogated by the dietary antioxidant curcumin. *Food and Chemical Toxicology 50*: 641–647.

Song, M., Yuan, S., Yin, J., Wang, X., Meng, Z., Wang, H. & Jiang, G. (2012). Size-dependent toxicity of nano-C60 aggregates: more sensitive indication by apoptosis-related Bax translocation in cultured human cells. *Environmental science & technology 46*: 3457-3464.

Sousa, C. A., Soares, H. M. & Soares, E. V. (2018). Nickel oxide (NiO) nanoparticles disturb physiology and induce cell death in the yeast Saccharomyces cerevisiae. *Applied Microbiology and Biotechnology 102*: 2827-2838.

Takle, S. P., Naik, S. D., Khore, S. K., Ohwal, S. A., Bhujbal, N. M., Landge, S. L., Kale, B. B. & Sonawane, R. S. (2018). Photodegradation of spent wash, a sugar industry waste, using vanadium-doped TiO 2 nanoparticles. *RSC Advances 8*: 20394-20405.

Vallet-Regí, M., Colilla, M., Izquierdo-Barba, I. & Manzano, M. (2018). Mesoporous silica nanoparticles for drug delivery: current insights. *Molecules 23*: 47-55.

Vissers, C., Ming, G.-l. & Song, H. (2019). Nanoparticle technology and stem cell therapy team up against neurodegenerative disorders. *Advanced drug delivery reviews* 1:1-10

Vitali, M., Rigamonti, V., Natalello, A., Colzani, B., Avvakumova, S., Brocca, S., Santambrogio, C., Narkiewicz, J., Legname, G. & Colombo, M. (2018). Conformational properties of intrinsically disordered proteins bound to the surface of silica nanoparticles. *Biochimica et Biophysica Acta (BBA)-General Subjects 1862*: 1556-1564.

Ye, Y., Liu, J., Xu, J., Sun, L., Chen, M. & Lan, M. (2010). Nano-SiO2 induces apoptosis via activation of p53 and Bax mediated by oxidative stress in human hepatic cell line. *Toxicology in Vitro 24*: 751-758.

Zeinabad, H. A., Zarrabian, A., Saboury, A. A., Alizadeh, A. M. & Falahati, M. (2016). Interaction of single and multi wall carbon nanotubes with the biological systems: tau protein and PC12 cells as targets. *Scientific Reports 6*: 26508-18.

Zhu, Y., Eaton, J. W. & Li, C. (2012). Titanium dioxide (TiO2) nanoparticles preferentially induce cell death in transformed cells in a Bak/Bax-independent fashion. *PloS one 7*: 50607-620.

Zikeli, F., Vinciguerra, V., Taddei, A. R., D'Annibale, A., Romagnoli, M. & Mugnozza, G. S. (2018). Isolation and characterization of lignin from beech wood and chestnut sawdust for the preparation of lignin nanoparticles (LNPs) from wood industry side-streams. *Holzforschung 72*: 961-972.

Zolghadri, S., Saboury, A., Golestani, A., Divsalar, A., Rezaei-Zarchi, S. & Moosavi-Movahedi, A. (2009). Interaction between silver nanoparticle and bovine hemoglobin at different temperatures. *Journal of Nanoparticle Research 11*: 1751-59.

Table 1. Different contents of secondary structure of Hb either alone or with different concentration of NiO NPs

Concentration of NPs	α-helix (%)	β-sheets (%)	Turn/ loop (%)	Random coil (%)
0	66.02	14.88	9.01	10.09
0.01	65.51	14.58	9.25	10.66
0.05	58.08	13.21	11.03	17.68
0.1	54.81	12.58	12.21	20.40

Figure 1. UV-Vis spectra of Hb either alone (red) or with different concentrations of NiO NPs 0.01 mg/ml (green), 0.05 mg/ml (purple), and 0.1 mg/ml (blue).

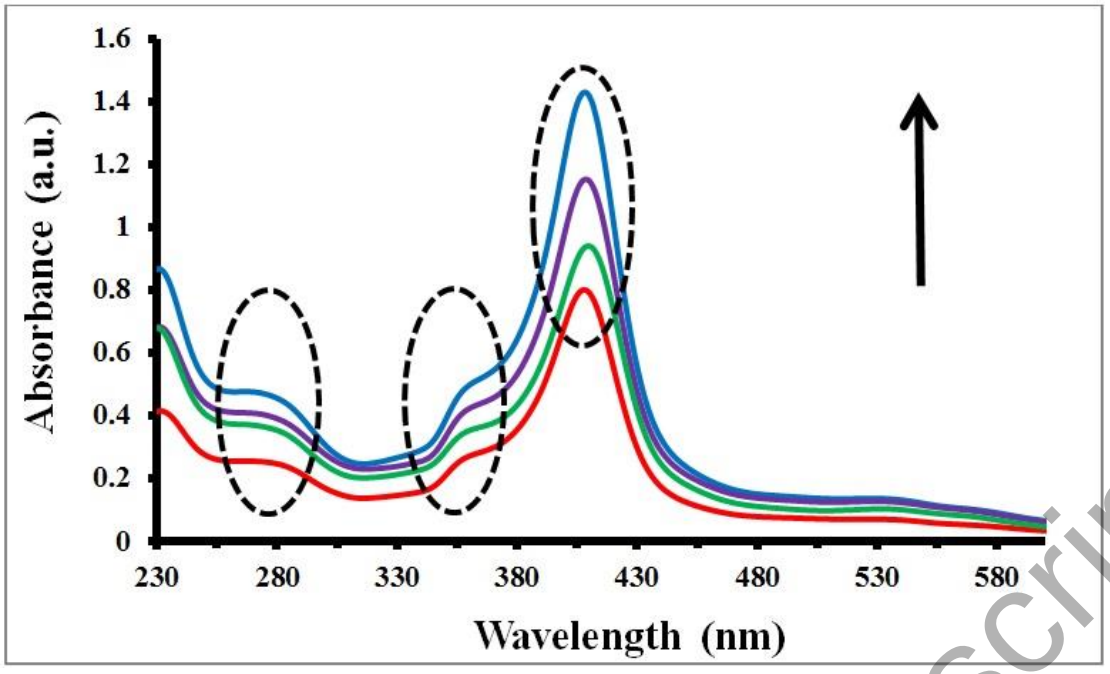

Figure 2. Fluorescence spectra of Hb with an excitation emission of 325 nm (a) and 465 nm (b) in the absence (red) and presence of NiO NPs with different concentrations of 0.01 mg/ml (green), 0.05 mg/ml (purple), and 0.1 mg/ml (blue).

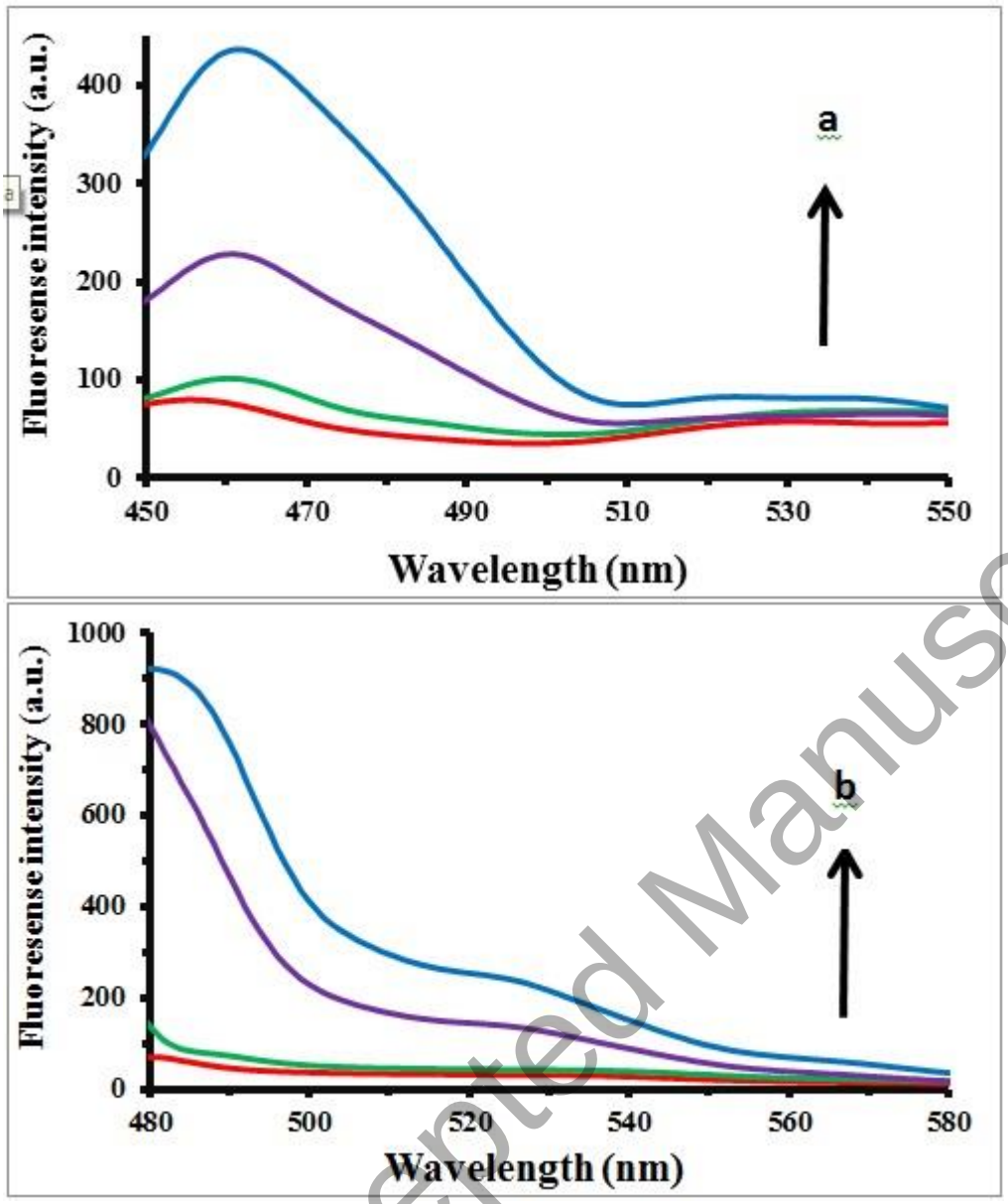

Figure 3. The Far UV-CD (190-260 nm) bands of Hb in the absence (red) and presence of NiO NPs with different concentrations of 0.01 mg/ml (green),0.05 mg/ml (purple), and 0.1 mg/ml (blue).

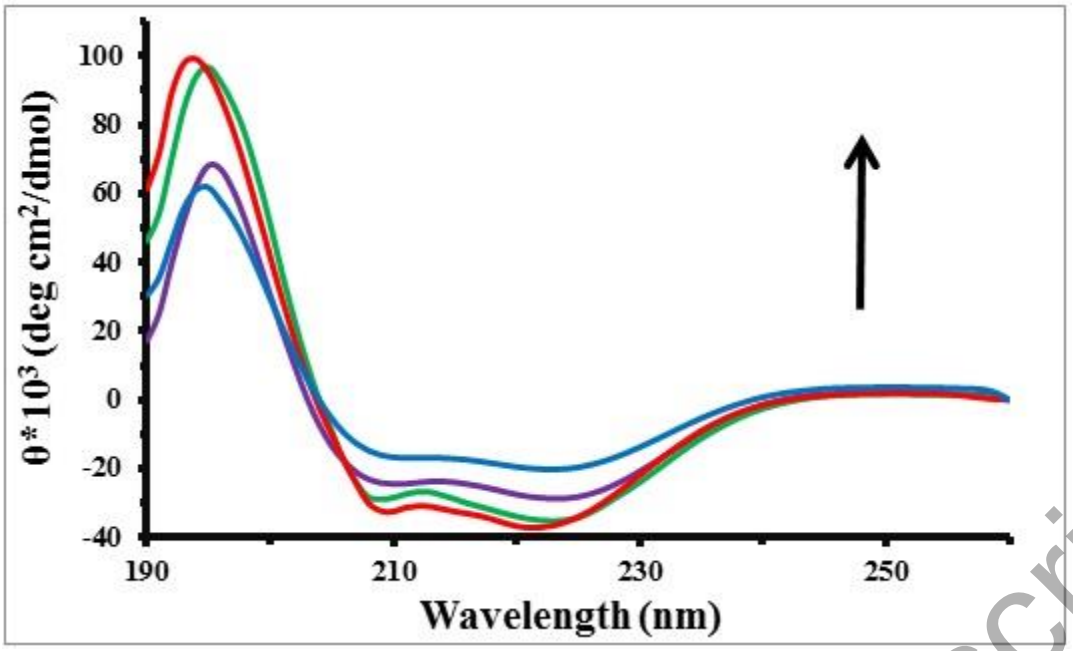

Figure 4. The near UV-CD (260-350 nm) bands of Hb either alone (red) or with NiO NPs with different concentrations of 0.01 mg/ml (green), 0.05 mg/ml (purple), and 0.1 mg/ml (blue).

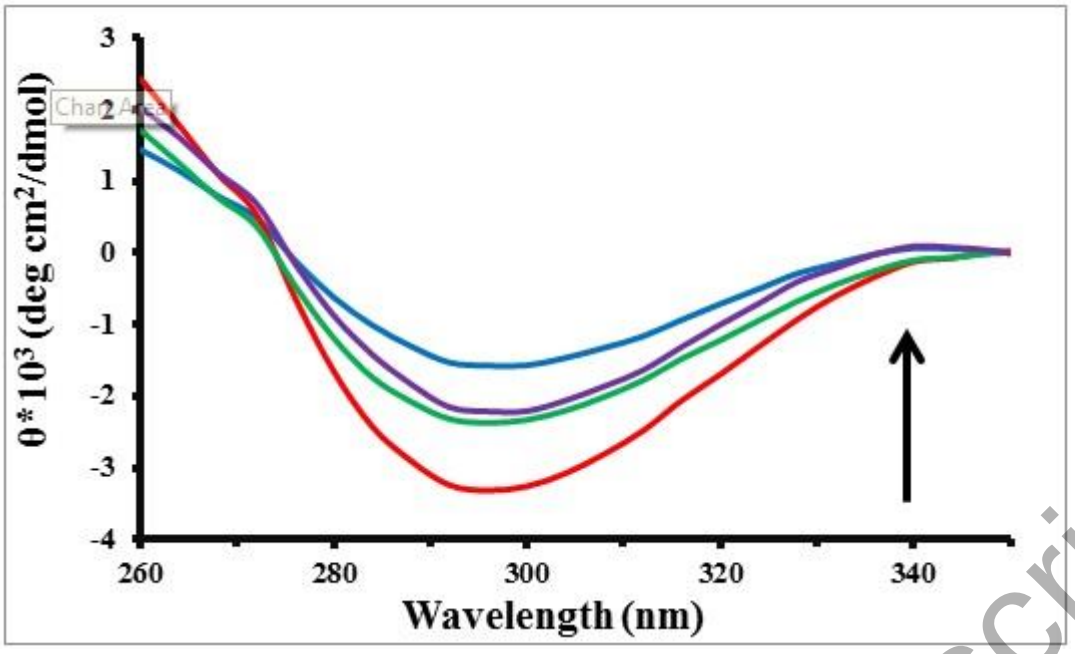

Figure 5. The near UV-CD (380-440 nm) bands of Hb in the absence (red) and presence of NiO NPs with different concentrations of 0.01 mg/ml (green),0.05 mg/ml (purple), and 0.1 mg/ml (blue).

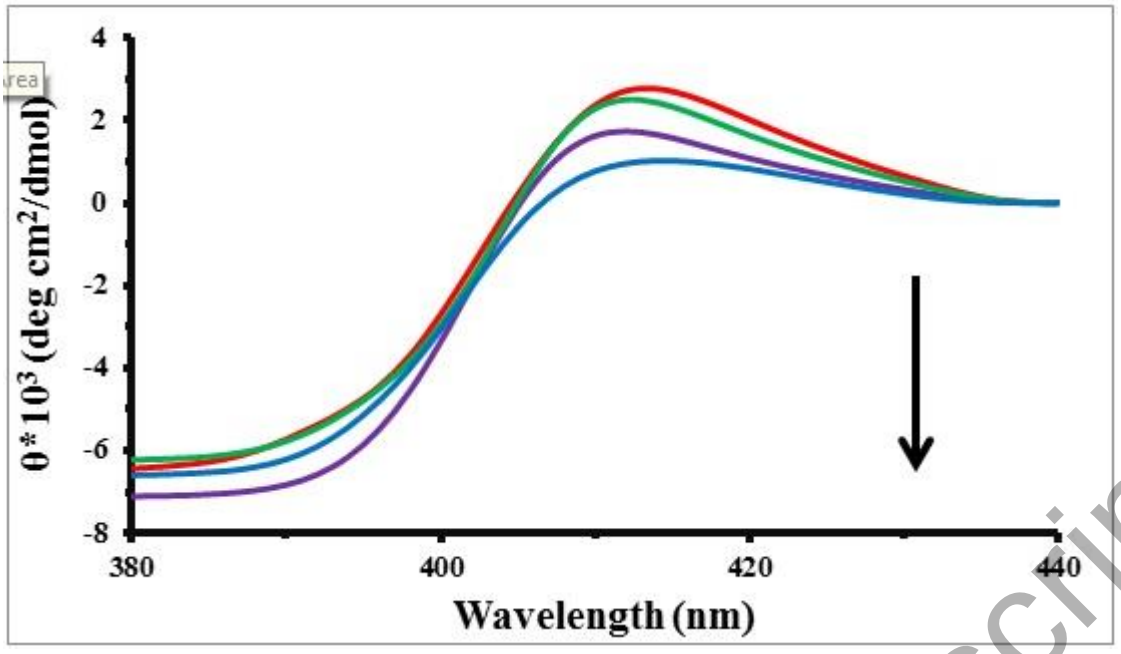

Figure 6. The side view of molecular modelling in the beginning (a) and after the interaction of Hb with NiO slab (b). The top view in the beginning (c) and after the interaction of Hb with NiO nanocluster (d)

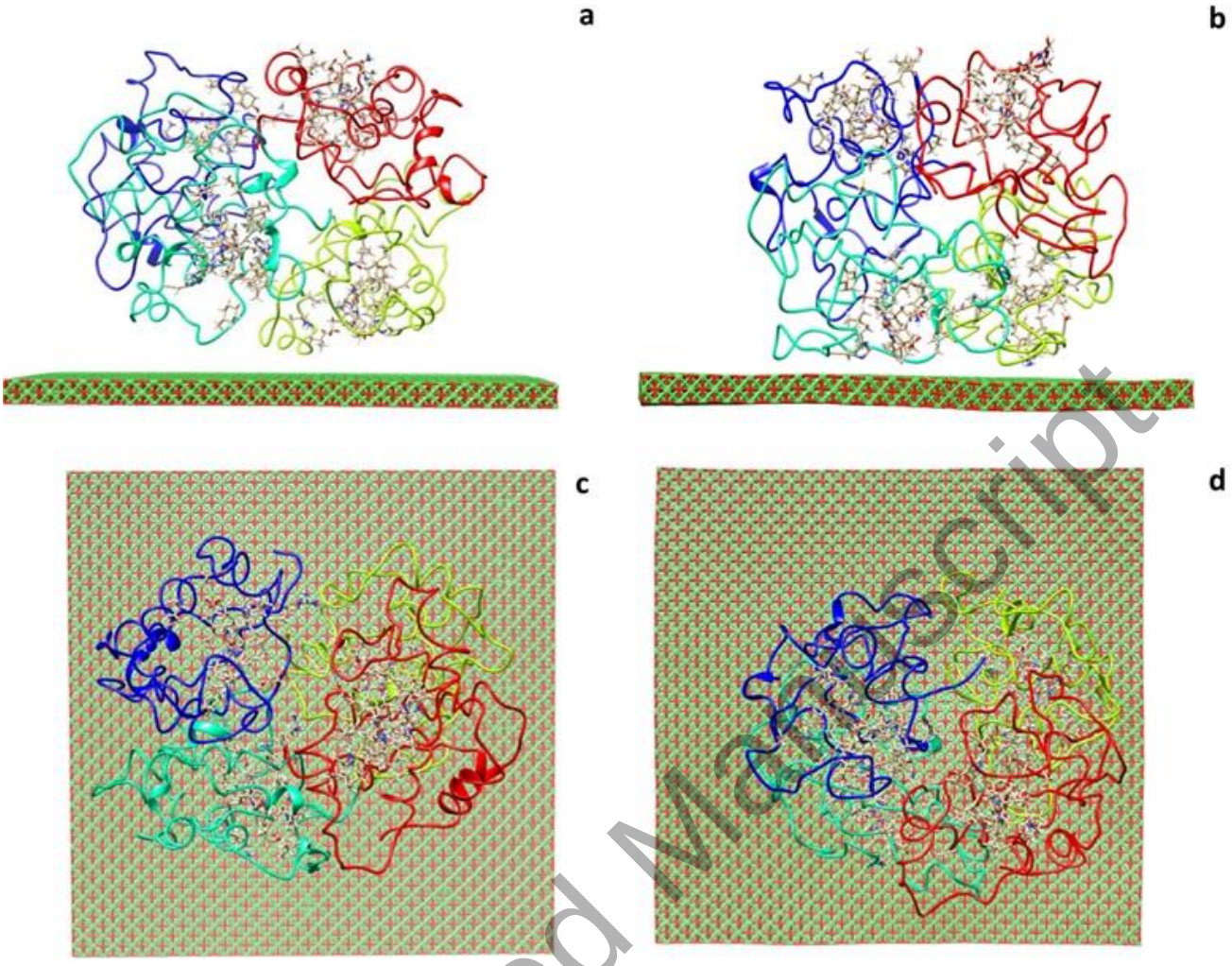

Figure 7. The molecular modelling of heme group at the beginning (a) and after interaction of Hb with NiO slab (b).

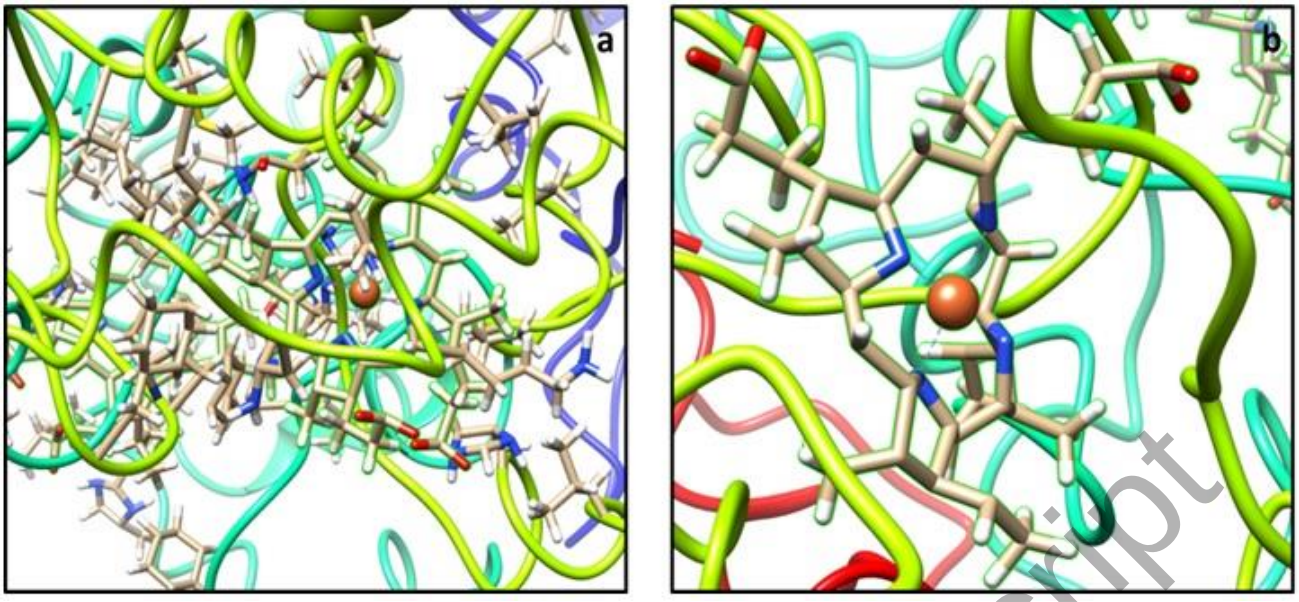

Figure 8. ThT fluorescence spectra of Hb in the absence (red) and presence of NiO NPs with different doses of 0.01 mg/ml (green), 0.05 mg/ml (purple), and 0.1 mg/ml (blue).

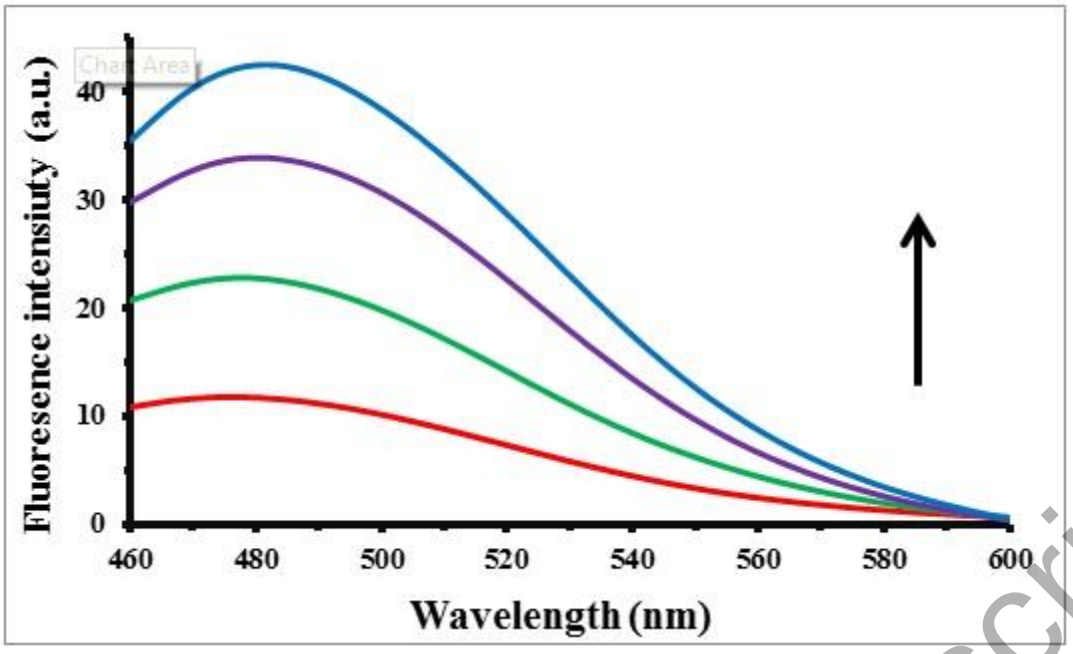

Figure 9. TEM images of Hb solution (a), NiO NP solution (b) and NiO/Hb complex solution(c).

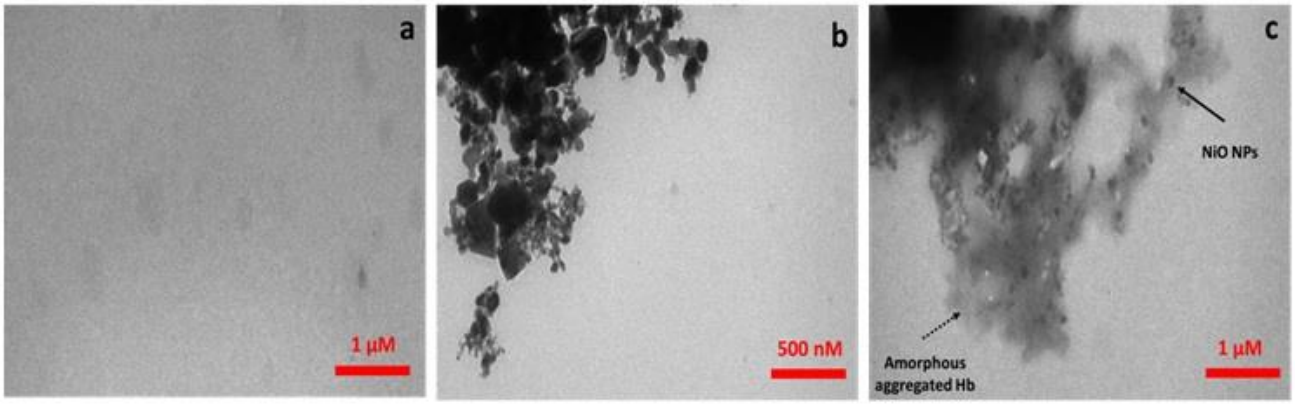

Figure 10. MTT assay of lymphocyte cells after treating with different doses of NiO NPs. **P*-value <0.05 and ***P*-value <0.01, relative to the negative control group

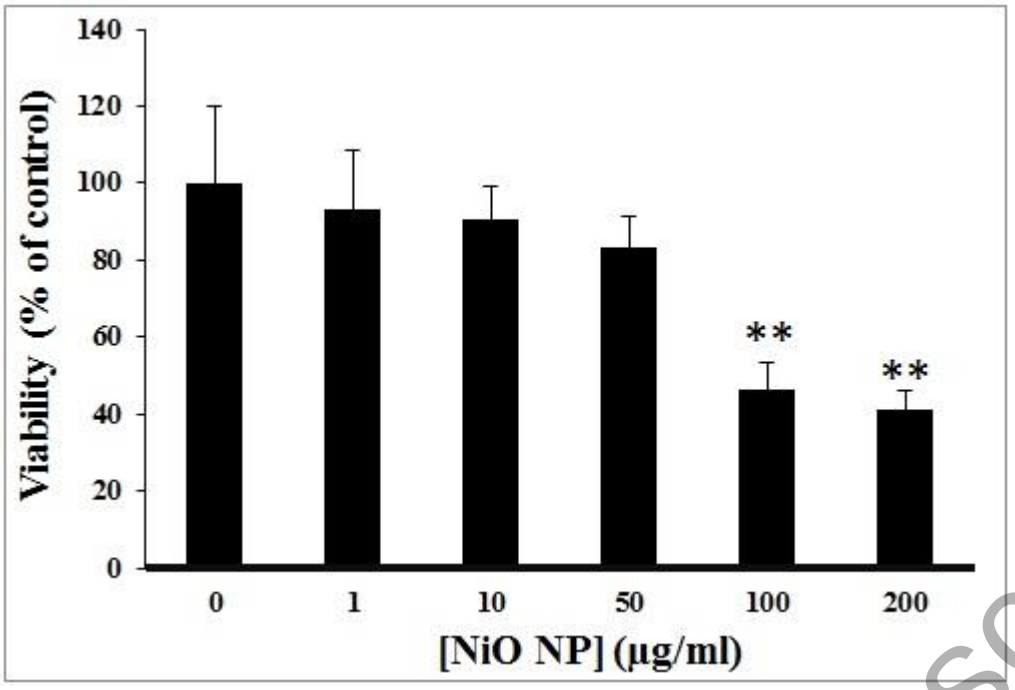

Figure 11. DAPI staining of cells exposed to varying doses of NiO NPs (0 [A], 1 [B], 10 [C], 50 [D], 100 [E] and 200 µg/ml [F]) for 24 hr.

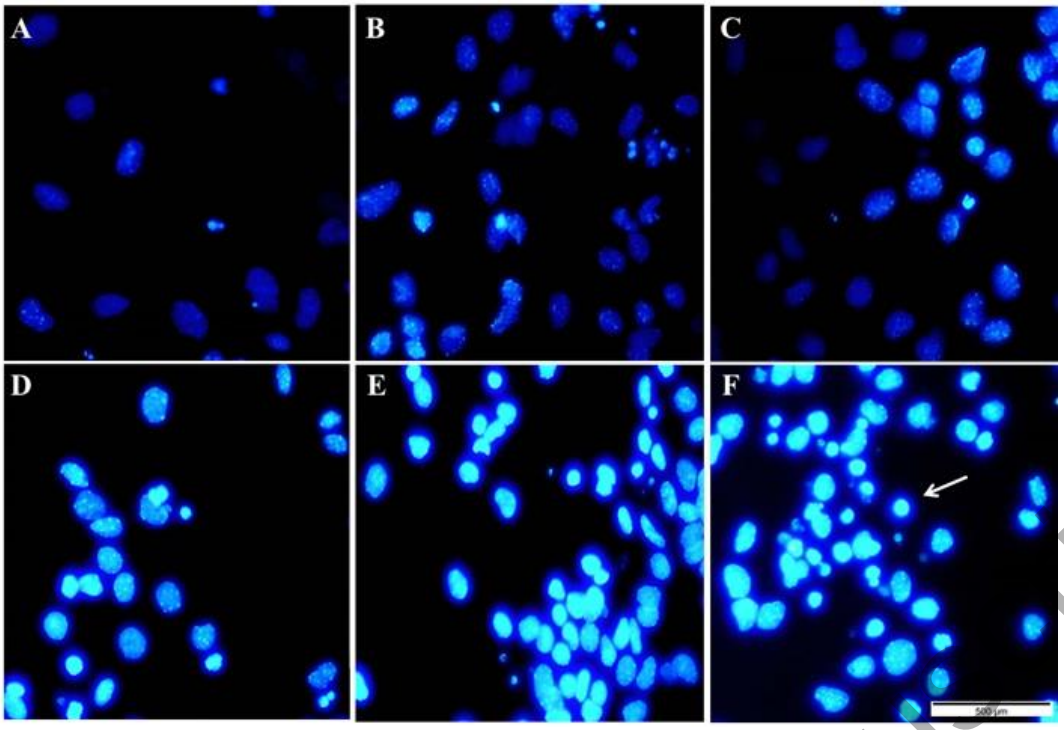

Figure 12. Bax, Bcl-2 and Bax/Bcl-2 mRNA expression at IC_{50} concentrations of NiO NPs for 24 hr. **P*-value <0.05 relative to the negative control group.